Electronic Supplementary Information to:

Long-period and High-stability Three-dimensional Surface-enhanced Raman Scattering Hotspot Matrix

Meihong Ge,[a,b] Pan Li,[a]* Chentai Cao,[a,b] Shaofei Li,[a] Dongyue Lin,[a,b] Liangbao Yang[a]*

Center of Medical Physics and Technology, Hefei Institutes of Physical Science, Chinese Academy of Sciences, Hefei 230031, China.

Department of Chemistry, University of Science & Technology of China, Anhui, Hefei 230026, China.

* Correspondence and requests for materials should be addressed to L. B. Yang (E-mail: lbyang@iim.ac.cn).

A. EXPERIMENTAL SECTION

2.1. Reagents

Nodularin was purchased from Enzo Life Sciences. Solid nodularin toxin was dissolved to 0.05 g/L in water and stored at −20 °C until analysis. Silver nitrate, sodium citrate, potassium iodide, and glycerol were bought from Shanghai Chemicals Company. All the chemicals used were of analytical grade or better and were used without further purification. Ultrapure water (>18.0 MΩ·cm) was prepared using a Millipore Milli-Q gradient system throughout the experiment.

2.2. Apparatus

An inverted microscope (eclipse Ti−U, Nikon, Japan) equipped with a dark-field condenser (0.8 < NA < 0.95) and a 40×objective lens (NA = 0.8) was used by Prof. Long's group (ECUST, Shanghai) for the real-time monitoring of the morphological alterations of particle aggregates in Ag sols.[1] A VIS miniature optical fiber spectrometer (Insion, Germany) was used by Prof. Du's group (ECUST, Shanghai) for the time-dependent visible diffuse reflection absorption spectra of 5 μL droplet.[2] Raman spectra were performed on a Lab-RAM HR800 spectrometer with a 633 nm laser excitation source.

2.3. Preparation of iodide-stabilized silver nanoparticles (Ag ISNP).

The Ag sols were prepared in accordance with the method of Lee and Meisel.[3] In brief, 1 ml of 0.1 M $AgNO_3$ was added to 99 ml of Milli-Q water (18.2 MΩ·cm), and heated to 100 °C; 4 ml of 1% sodium citrate was added to the boiling solution under vigorous stirring. The solution was kept boiling for ~1 h. This procedure resulted in a gray-yellow solution. The Ag sols were first washed once; centrifugation of 1000 μL of Ag sols at 8000 r for 10 min was then performed, and 997 μL of the colorless supernatant was discarded. The remaining 3 μL, which contained a black pellet was re-dispersed under sonication. The Ag ISNP was prepared in accordance with the method of Ren.[4] In brief, the remaining 3 μL Ag NPs was mixed with an equal volume of 1 mM potassium iodide, which was incubated for 20 min at 25 °C to ensure a complete modification of the surface of Ag NPs with iodide. After that, the Ag ISNPs were mixed with an equal volume of ten times diluted glycerol aqueous solution at room temperature for SERS measurements.

2.4 SERS measurements and data processing

As illustrated in Fig. S1, a sample droplet was placed on the surface of the silicon wafer. The laser spot was focused on the substrate surface and centered at the top point of this droplet. Time-course SERS mapping was then performed. For all SERS spectra, baseline correction was performed using

the LabSpec V5.58.25 software, and the peak frequency and FWHM were obtained from peak fitting.

2.5 Zeta potential measurements

The Zeta potential of each sample was recorded using a Zetasizer Nano ZS Instrument (Malvern, UK) at 25 C. Each sample was determined with five independent measurements, and each measurement was repeated three times.

2.6 Dark-field spectrum measurements

Dark-field spectrum measurements were conducted using an inverted microscope (eclipse Ti-U, Nikon, Japan) equipped with a dark-field condenser ($0.8 < NA < 0.95$) and a 40x objective lens ($NA = 0.8$), which was provided by Prof. Long's group (East China University of Science and Technology, Shanghai). A 100-W halogen lamp provided white light to excite the NPs and generate plasmon resonance scattering light. The dark-field color images were acquired using a true-color digital camera (Nikon DS-fi).

2.7 Time-dependent visible diffuse reflection absorption spectrum measurements

For in situ time-dependent visible diffuse reflection absorption spectrum measurements, the droplet to be measured was placed on a transparent fluorosilylated quartz slide, which was then placed on the top of an optics-integrating sphere. An aluminized mirror was then used to reflect the incident light back to the optics-integrating sphere. The light from the integrating sphere passed through the sample twice and then returned to the sphere. The light and sample backgrounds could be deducted easily and simultaneously. The time-resolved optical behavior of the colloids could be precisely followed.

2.8 SEM measurements

The scanning electron microscopy (SEM) images were taken by an Auriga focused ion-beam scanning electron microscopy (FIB-SEM), equipped with X-ray energy dispersive spectroscopy (EDS) capabilities, operated at an acceleration voltage of 15 kV.

2.9 UV-Vis absorption spectrum measurements

Ultraviolet–visible (UV-vis) spectrum were performed on a Cary 5000 Varian UV-vis spectrometer and recorded at the range of 200-800 nm, corrected against the background spectrum, and normalized to zero absorbance at 800 nm.

B. Additional Figures

The schematic illustration of experimental flow is shown as Fig. S1. First, the concentrated Ag sols mixed with iodide with an equal volume of 1 mM potassium iodide, which was incubated for 20 min at 25 °C to ensure a complete modification of the surface of Ag NPs with iodide. The resulting solution is then mixed in equal proportions with glycerol aqueous solution for D-SERS experiment.

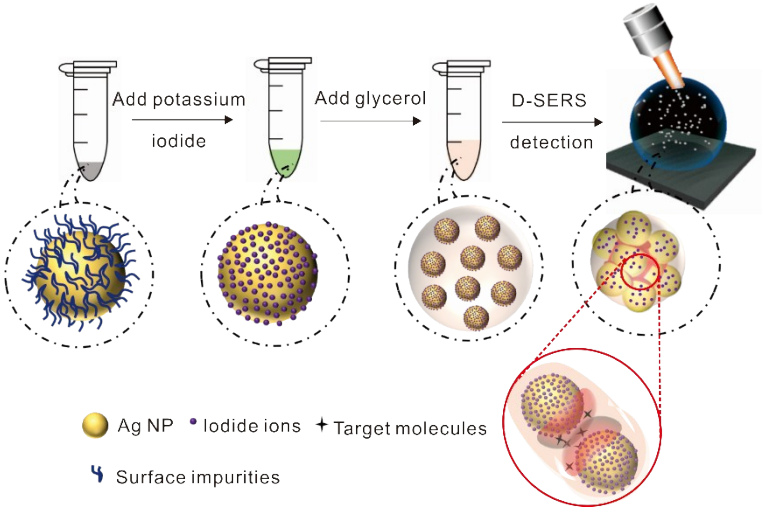

Fig. S1 Schematic illustration of experimental flow.

The surface impurities of silver nanoparticles have a strong background signal, which will interfere with the detection of the object to be tested. In accordance with the method of Ren, [4] we effectively remove the surface impurities of Ag NPs and obtain the Ag ISNP. Fig. S2 shows the SERS spectra of Ag NPs before and after treatment with potassium iodide, it is obvious that the impurity peaks on the surface of the silver nanoparticles disappear after treatment.

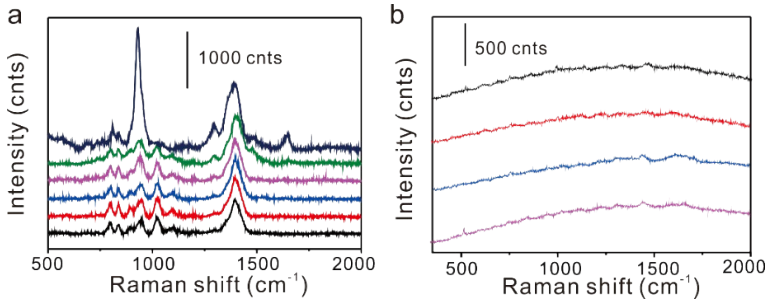

Fig. S2 SERS spectra of Ag NPs before (a) and after (b) treatment with potassium iodide.

Further, effects of glycerol on the plasmonic properties of the long-period and high-stability 3D SERS hotspot matrix were investigated. Dependence of the SERS enhancement on glycerol concentration was presented in Fig. S3a-c, represent 3%, 5% and 10% glycerol solutions, respectively. The intensities of 1616 cm^{-1} peaks were counted in Fig. S3d. Through comparison, it was found that 5% concentration glycerol had better plasmonic properties.

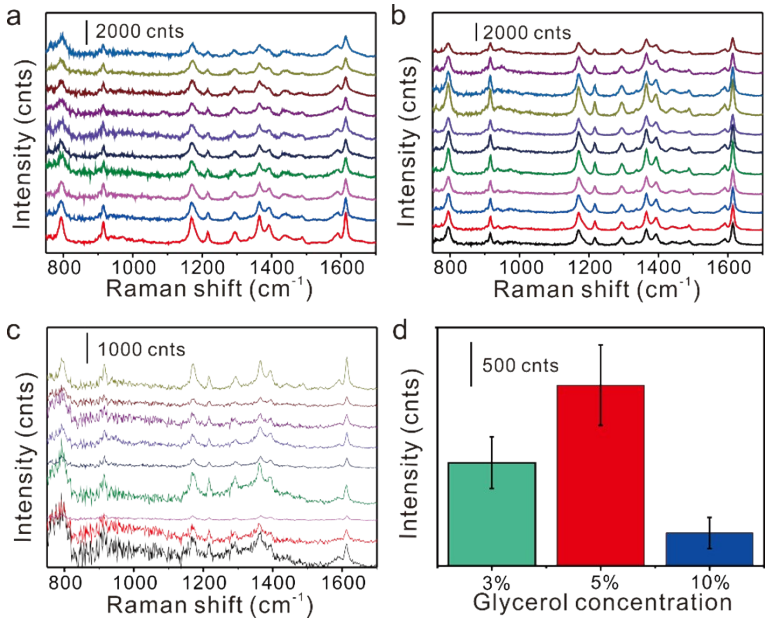

Fig. S3 SERS spectra of 10^{-6} M MG obtained at different concentrations of glycerol, (a) 3%, (b) 5% and (c) 10%, (d) comparison of plasmonic properties of the three concentrations at the characteristic peak of MG at 1616 cm^{-1}.

To further discuss the plasmonic properties of the SERS hotspots in 5% concentration glycerol system, SERS spectra of MG with various concentrations were researched. As Fig. S4 shows, the critical factors for practical SERS analysis, sensitivity and detection limit, were characterized and obtained.

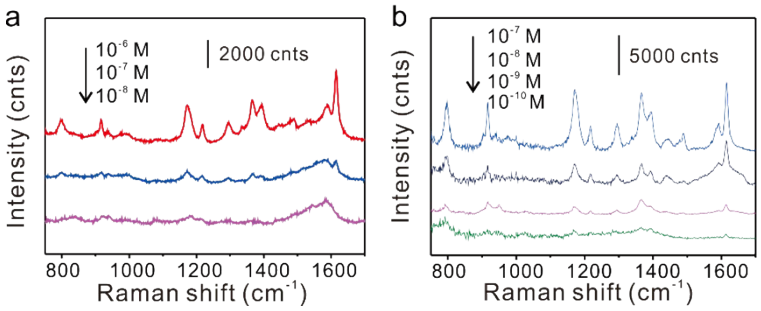

Fig. S4 SERS spectra obtained of MG with various concentrations from (a) 10^{-6}~10^{-8} M in water system and (b) 10^{-7}~10^{-10} M in glycerol system.

To further prove the plasmonic properties of the long-period and high-stability 3D SERS hotspot matrix, SERS spectra of 10^{-6} M MG at different time periods in the dynamic detection process were enumerated as Fig. S5 shown. MG signals can be detected efficiently almost in the whole dynamic detection process, which proves that the 3D hotspot matrix is effective and highly stable for at least 20 minutes. The time-dependent SERS mapping of the whole process is shown in Fig. S6.

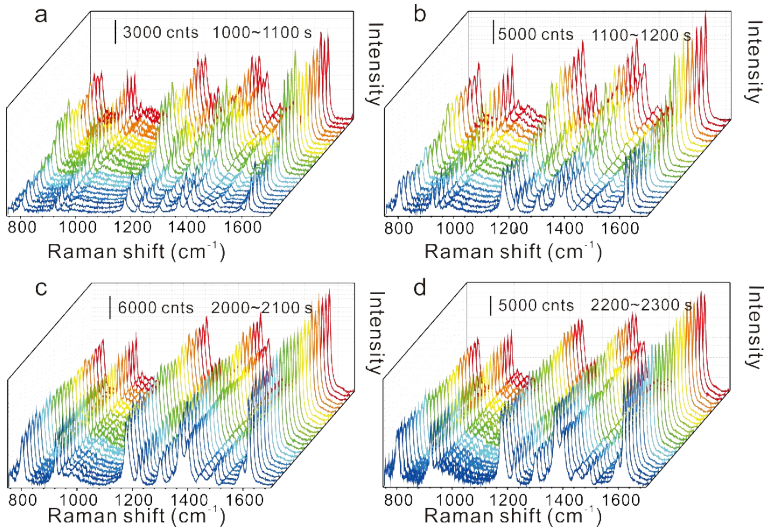

Fig. S5 SERS spectra obtained at different time periods in the dynamic detection process of 10^{-6} M MG, (a) 1000~1100 s, (b) 1100~1200 s, (c) 2000~2100 s and (d) 2200~2300 s.

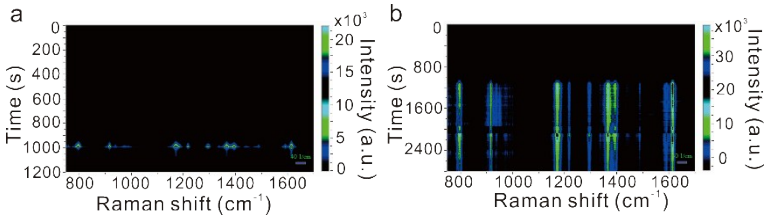

Fig. S6 Time-dependent Raman spectra of 10^{-6} M MG. Continuous time-dependent SERS mapping from (a) 0 to 1200 s in water system and (b) 0 to 3000 s in glycerol system.

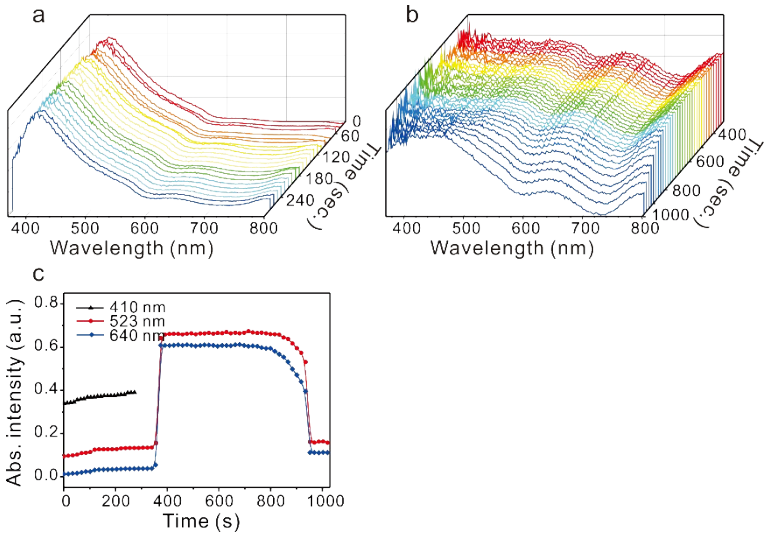

Fig. S7 Time-dependent visible diffuse absorption spectra of silver in water system during the evaporation process of a 3 μL sample, (a) 0~300 s, (b) 300~1200 s, (c) the value of absorbance intensity of peak at 410 nm, 523 nm and 640 nm.

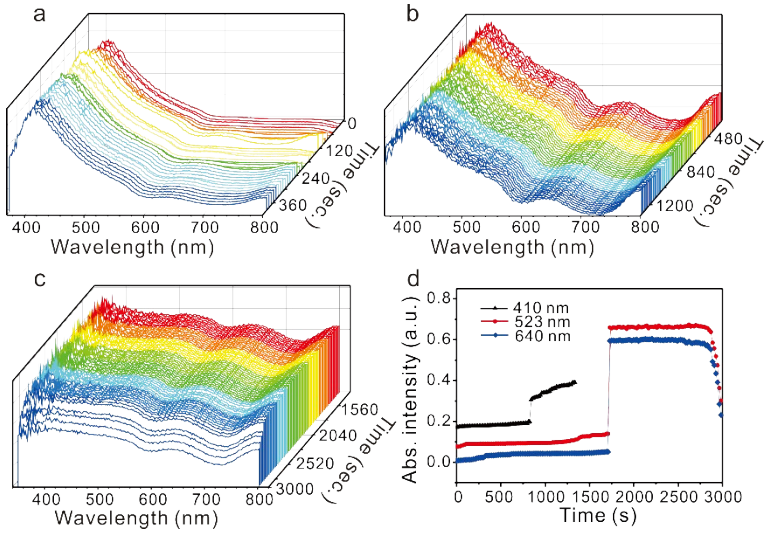

Fig. S8 Time-dependent visible diffuse absorption spectra of silver in water system during the evaporation process of a 3 μL sample, (a) 0~360 s, (b) 360~1200 s and (c) 1200~3000 s, (d) the value of absorbance intensity of peak at 410 nm, 523 nm and 640 nm.

To experimentally compare the persistence of hotspots with the glycerol system, the time-dependent Raman spectra of different molecules, (a)NOD, (b) TBZ and (c)MAMP by the traditional 3D hotspot matrix in water system were collected. Hotspots last only a few dozen seconds, which is much shorter than the glycerol system.

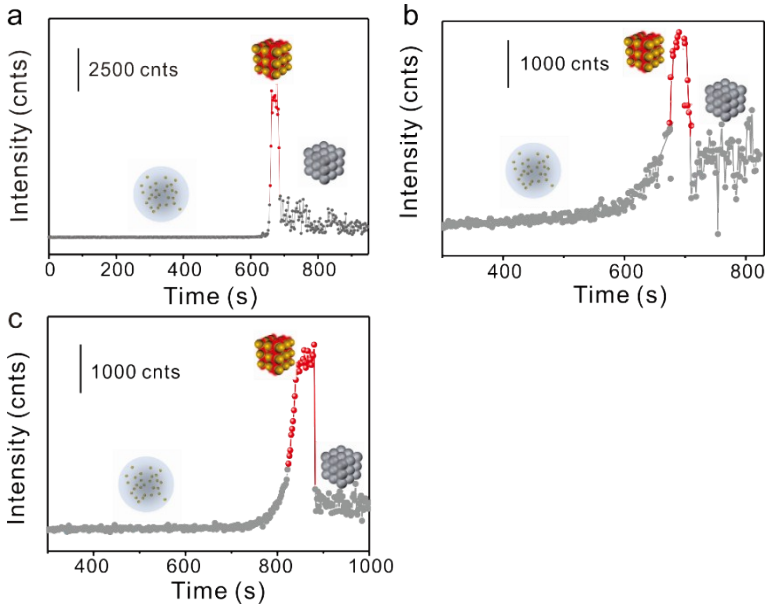

Fig. S9 Time-dependent Raman spectra of different molecules, (a)NOD, (b) TBZ and (c)MAMP by the traditional 3D hotspot matrix in water system.

To test characterize the time of 3D hotspot matrix in the glycerol system, we tested 10^{-7} M MG in 5% glycerol system at different time periods. As Fig S10 shown, the SERS fingerprint characteristic peaks of MG were still intact after 24 h with some reduction in intensity. It demonstrates the protective effect of such a glycerol system on 3D hotspot matrix.

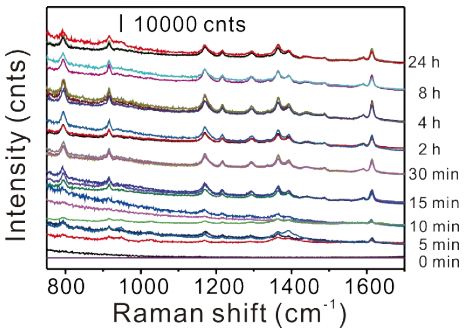

Fig. S10 SERS spectra obtained at different time periods of 10^{-7} M MG in 5% glycerol system.

Fig. S11 shows the SEM images and UV-Vis of the Ag NPs used in the experiment. The average size of Ag NPs is between 60 and 70 nm, and the UV-Vis absorption peak is 410 nm.

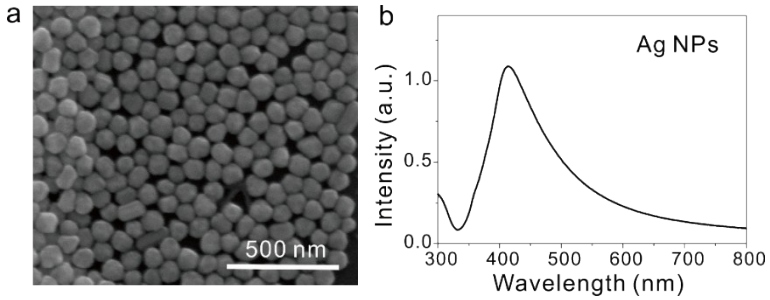

Fig. S11 Characterizing of the Ag NPs. (a) SEM image and (b) UV-Vis absorption spectrum of Ag NPs.

References

1. L. Shi, C. Jing, W. Ma, D. Li, J. E. Halls, F. Marken and Y. Long, *Angew. Chem. Int. Ed.*, 2013, **52**, 6011-6014.
2. Y. Kang, T. Wu, W. Chen, L. Li and Y. Du, *Food Chem.*, 2019, **270**, 494-501.
3. P. C. Lee and D. Melsel, *J. Phys. Chem.*, 1982, **86**, 3391-3395.
4. L. Xu, C. Zong, X. Zheng, P. Hu, J. Feng and B. Ren, *Anal. Chem.*, 2014, **86**, 2238-2245.